



An in-and-out-the-lab Raman spectroscopy study on street art murals from Reggio Emilia in Italy

Anastasia Rousaki¹ , Peter Vandenabeele^{1,2} , Michela Berzioli³, Ilaria Saccani⁴, Laura Fornasini⁵ , Danilo Bersani^{6,a}

¹ Raman Spectroscopy Research Group, Department of Chemistry, Ghent University, Krijgslaan 281 (S-12), 9000 Ghent, Belgium

² Archaeometry Research Group, Department of Archaeology, Ghent University, Sint-Pietersnieuwstraat 35, 9000 Ghent, Belgium

³ AN.T.A.RES srl, Via Aldo Moro, 24/a, 40068 San Lazzaro di Savena, BO, Italy

⁴ CESMAR7- Centro per lo Studio dei Materiali Per il Restauro APS, Viale dei Mille 32, 42121 Reggio Emilia, Italy

⁵ ICCOM-CNR, Institute of Chemistry of Organometallic Compounds, National Research Council, Via G. Moruzzi, 1, 56124 Pisa, Italy

⁶ Dipartimento di Scienze Matematiche, Fisiche e Informatiche, Università di Parma, Parco Area delle Scienze 7/A, 43124 Parma, Italy

Received: 8 July 2021 / Accepted: 25 January 2022

© The Author(s) 2022

Abstract The street art murals ‘The Big Mother’ by Gola Hundun, the ‘Big Sacral Bird’ by Kenor, the ‘Oriental Carpet’ by H101 and ‘The Economy Subdues You’ by Zosen, belonging to the Cooperative Popular Houses of Mancasale and Coviolo in Reggio Emilia (Italy), were investigated by the use of various mobile Raman spectrometers coupled to different lasers and by micro-Raman spectroscopy on selected samples. The study was made necessary by the evident fading of many colours, despite the young age of the paintings, realized in 2010. The first step of the investigation, realized by the on-site campaign, was the identification of the materials, and in particular of the dyes. The main chromophores were identified as polycyclic, monoazo- and disazo- organic pigments, with inorganic compounds as bismuth vanadate (BiVO_4) together with the extensive presence of rutile (TiO_2). The second step was devoted to the study of the degradation mechanism affecting the colourful layers of the murals. It required the use of laboratory micro-spectrometers and was carried out on a reduced set of samples, selected during the in-situ campaign. This combination of on-site and laboratory Raman spectroscopy allowed the obtaining of the complete identification of the palette used by the different artists in a single day of measurements, in a complete non-destructive way. In addition, it was possible to minimize the number of samples required for the study of the degradation process.

1 Introduction

Outdoor artworks of contemporary public art are usually realized with modern synthetic materials which suffer from lack of long-last stability, producing alteration effects and deterioration problems according to their chemical composition. Furthermore, the exposure to severe and extreme weather conditions and environmental pollution are crucial issues to be considered in the conservation and protection of these artifacts.

For these reasons, a lot of attention has been recently paid to the investigation of the mechanical state of conservation of contemporary outdoor artworks and their aesthetic alterations [1–9].

The three-year European project “Conservation of Art in Public Spaces” (CAPuS), involving 15 partners among universities, academies, companies and research centres, is designed to study artworks of contemporary public art, including murals and outdoor sculptures. The CAPuS project, co-funded by the ERASMUS + Knowledge Alliances 2018–2021 programme, aimed at contributing to the dissemination of knowledge in the field of public art conservation. In particular, the CAPuS project has developed specific conservation guidelines for artworks in public spaces together with an innovative training module for higher education institutions as well as an open e-learning module for professionals [10]. An illustrated multi-lingual glossary providing definitions in street art and conservation, and an open-access digital repository containing subpages of selected artworks and specific details (i.e. materials analysis, condition reports, and general archival documentation) have been also realized and constantly implemented during project lifespan and beyond [11]. The characterization of artworks materials and their degradation processes is of fundamental importance to the development of conservation treatment protocols. Within the project, the Italian partners focused on works of *post muralism* and *street art* to first study the compositional materials and their characteristic degradation processes and later develop specific conservation methods. The data acquired during in situ campaigns contributed to the formalization of conservation guidelines, as well as to the creation of formative modules for students and professionals.

^a e-mail: danilo.bersani@unipr.it (corresponding author)

This work describes the research carried out on murals belonging to the Cooperative Popular Houses of Mancasale and Coviolo in Reggio Emilia (Italy), realized on buildings constructed during the late-1950s by the Italian-Spanish collective *Proyecto Ritual* in 2010. The analyses were carried out on the murals “The Big Mother” by Gola Hundun, “Big Sacral Bird” by Kenor, “Oriental Carpet” by H101 and “The Economy Subdues You” by Zosen [12, 13]. In these murals the importance of the man-nature relationship is emphasized, being one of the main characteristic themes of the undivided workers’ houses since their foundation in 1909, which were designed as housing focused on a self-subsistence economy [14, 15].

Opposite to the relatively good mechanical conservation state of the murals, a clear chromatic deterioration occurred. The south-facing orientation of some of the murals without any protection from the sun is critical for the degradation processes induced by the exposure to sunlight and weathering [1, 5, 16, 17]. The main effects consist of total or partial colour fading, a chromatic alteration manifested as the weakening of chroma, resulting from chemical reactions or exposure to direct sunlight [11], and other colour shifts, causing the loss of original contrast and therefore the readability of details. The commercial formulations used by the artists were cheap and easy to use paints that allow to paint quickly and with great impact on large formats without an important interest in conservation over time. These formulations are very complex mixtures of binding media, dyes, extenders, and additives mainly of organic nature at low resistance to degradation. Recurring alterations in some colours were also observed [18–21]. Some details are clearly visible in Fig. S1 (supplementary material). Furthermore, cracking with flaking, losses with crack pattern and efflorescence between the ground layer and the plaster occurred in some of the murals [20, 22].

Due to these chromatic alteration and deterioration effects, an in situ campaign with portable Raman spectrometers has been performed, to characterize the colorants involved in these phenomena. Raman spectroscopy was chosen as a fast, non-destructive technique, suitable for in situ use [23–26]. Raman spectra allow to uniquely identify organic and inorganic dyes and inorganic pigments. The use of three different instruments, with different excitation wavelengths, is useful to reduce the negative effect of fluorescence on the identification [23]. Moreover, in some cases it allowed us to take advantage of possible resonance effects, promoting the identification of both the colour palette and the alteration products [9, 17]. Thus, this study shed light on the deterioration mechanisms in the investigated outdoor artworks. In general, Raman spectroscopy had already proven to be a valuable tool for the investigation of synthetic organic pigments (SOPs) used in modern and contemporary art and on street art murals [9, 16, 27–34].

Numerous strategies have been employed regarding the identification of synthetic organic pigments. Brostoff et al. in 2009 [35] used micro-Raman spectroscopy, micro-X-ray diffraction (μ XRD) and X-ray diffraction (XRD) to study various forms of synthetic organic pigments as powders (measured as received by the manufacturer), stratified layers, and artists paints, in different media. Although XRD is underlined as a promising complementary technique for the identification of SOPs, the characterization of SOPs in oil paints was considered difficult. Quillen Lomax in 2010 [36] similarly concluded that XRD is of little use when SOPs are present in oil or gum. Saverwyns in 2010 [37] employed micro-Raman spectroscopy on paintings attributed to Liubov Popova. The technique was proven a valuable tool especially for the analysis of SOPs. The study demonstrated the chronological misplacement of the paintings and concluded that the paintings were faulty attributed to the artist. Russel et al. in 2011 [38] study the potentials (discussing problematics) of pyrolysis–gas chromatography–mass spectrometry (Py-GC–MS) for analysis of SOPs as pigments and SOPs in paints and paintings. Defeyt et al. in 2012 [39] used XRD, attenuated total reflectance micro-Fourier transform infrared spectroscopy (μ -FTIR-ATR) and micro-Raman spectroscopy on copper phthalocyanine (CuPc) polymorphs measured as pigments and paints with different binders and in 2013 [40] combined micro-Raman spectroscopy and linear discriminant analysis (LDA) for the differentiation of CuPc polymorphs. Vagnini et al. in 2017 [41] employed a handheld Raman spectrometer coupled to fluorescence reduction technology (also used in the current research) and mobile, X-ray fluorescence (XRF) and reflection infrared systems, for the overall characterization of art with Raman spectroscopy used successfully for the analysis of SOPs (among others materials). Steger et al. in 2019 [42] combined portable Raman spectroscopy and diffuse reflectance infrared Fourier transform spectroscopy (DRIFTS) (handheld FTIR) for the molecular and non-invasive identification of SOPs found on glass reverse paintings. Ghelardi et al. in 2015 [3] reported the results of artificial ageing (photochemical) of SOPs by using colorimetric measurements, Py-GC–MS and FTIR-ATR. Next to the colour change, the application of the last two techniques, suggested alterations in the aged samples and carbonyl groups formation, respectively. Germinario et al. in 2016 [43] when studying the components included in spray paints, stated that generally micro-Raman spectroscopy gave more information regarding the inorganic pigments and SOPs (and extenders/fillers) compared to FTIR and Py-GC–MS. The last two techniques performed better on the binders’ characterization, providing some information on the organic/inorganic pigments, extenders and fillers. Combined FTIR (ATR and transmission) and nuclear magnetic resonance (NMR) were employed by Ciccola et al. in 2017 [44] to investigate the role of SOPs in the degradation of the Acrylem AC 33 binder under UVB influence. Two years later, the same thematic was investigated by Ciccola et al. [17], by adding micro-Raman spectroscopy to the previous protocol. Sundberg et al. in 2021 [45] performed an in-depth comparative study on the performance of Py-GC–MS, ultra-high pressure LC-PDA, UPLC-PDA-HRMS, and micro-Raman spectroscopy for the SOPs identification for art samples. In the case of characterization of materials found in street art murals, multiple techniques were employed, including Raman spectroscopy [9, 33].

In the current study we present the extensive in situ analysis of the street art murals together with the micro-Raman results in order, not only to identify the artists’ palette but also to understand possible degradation mechanisms that affect the outdoor murals.



Fig. 1 Mobile Raman spectroscopy was applied on the street art murals **a** ‘Big Sacral Bird’ and **b** ‘The Economy Subdues You’. The scaffold on a truck was used in order to reach the higher parts of the street murals; **c** The mobile Raman systems involved in the current study. Clockwise appearance: the dispersive *i-Raman*[®]EX portable system, the *Bravo* handheld Raman spectrometer, the handheld Raman analyzer *RaPort*. The *i-Raman*[®]EX is connected to a laptop and a portable battery; **d** The fibre-optics probehead of *i-Raman*[®]EX positioned against the region of interest; **e** The fixed optical head of *Bravo* positioned against the mural ‘The Big Mother’ (foreground) while the researchers are simultaneously investigated the graffiti ‘Sacral Bird’ with the *RaPort* handheld spectrometer (background)

2 Materials and methods

In situ Raman analysis was performed on the street murals ‘The Big Mother’ by Gola Hundun, ‘Big Sacral Bird’ by Kenor, ‘Oriental Carpet’ by H101, and ‘The Economy Subdues You’ by Zosen. All the mobile Raman spectrometers were brought simultaneously on the field, and the analyses were carried out directly on the colourful surfaces of the street murals without jeopardising the works of art. An aerial work platform was used to measure the big-sized murals ‘Big Sacral Bird’ and ‘The Economy Subdues You’ (Fig. 1a and b) (up to 15 m) while a ladder with no additional equipment was used for investigating the ‘Oriental Carpet’ and ‘The Big Mother’. During a single day of on-site analysis, 47 different colour regions have been analysed, covering all the different chromatic hues, apparently stable and unstable, painted both by spray and by roller, of the four wall paintings. Every region was analysed with at least two different spectrometers, in most cases with three spectrometers, repeating the measurements in different (usually 3) spots for each area. A huge amount of spectral data was obtained in a very short time, minimizing the impact on the environment and on the inhabitants of the buildings. The analysed points are reported in Fig. S2 (supplementary material), as well as with the hue changes of the different chromatic areas.

Some millimeter-sized samples were collected during the measurements by means of a scalpel from the positions indicated in Fig. S2 (supplementary material). Four of them were embedded in epoxy resin and polished. The as-obtained samples and the cross-sections were then analyzed by a micro-Raman spectrometer.

2.1 In situ and direct analysis

All the mobile Raman spectrometers used for the on-site analysis of the outdoor murals can be visualized in Fig. 1c.

2.1.1 The Bravo handheld Raman spectrometer (Bruker, Ettlingen, Germany)

The *Bravo* handheld Raman system is a dual laser (785 and 853 nm) compact spectrometer able to acquire spectra in an extended spectral region from 300 to 3200 cm^{-1} . The system is coupled to a CCD detector, its spectral resolution is 10–12 cm^{-1} and the laser power is fixed (less than 100 mW). This battery-operated spectrometer that weights 1.5 kg uses an automatic integrated calibration. *Bravo* is using the sequentially shifted excitation (patented) technology to reconstruct a spectrum that is free from fluorescence effects.

The *Bravo* Raman system is actually collecting slightly shifted Raman spectra from slightly different laser excitations produced by changing the lasers’ current. In practice, it uses two spectral regions; from 300 to 2200 cm^{-1} for the 785 nm laser and from 1200 to 3200 cm^{-1} for the 853 nm laser, to collect 3 shifted Raman spectra per laser per spectral region and reconstructs a 7th final spectrum free of fluorescence. In theory, if the differences in laser excitations are small (slightly different), the broad fluorescence features can remain unchanged while the actual Raman signal is shifted. The user can separately view all the spectra recorded together with the final one. This is very useful in cases where the in-built algorithm of the instrument produces artefacts other than the actual Raman bands.

All the measurements were conducted in the automatic mode bringing the plastic protective head (used to secure the lens/laser optics) of the fixed probehead of the spectrometer in contact with the surface under study. The working distance is defined at around 4 to 5 mm while the spot size is smaller than 1 mm (both as reported by the manufacturer).

2.1.2 The dispersive *i-Raman*® EX portable system (BWTEK, Newark, USA)

The *i-Raman*® EX is a fibre optics dispersive Raman spectrometer coupled to a 1064 nm laser and equipped with a TE-cooled InGaAs detector. The system records spectra in the spectral range from 100 to 2500 cm^{-1} , with a spectral resolution of 10 cm^{-1} . The adjustable laser power can reach up to 499 mW, while the main unit weighs 3.4 kg. The spectrometer is coupled to an external laptop, to allow for setting the experimental conditions and collecting the spectra. In general, the experimental conditions used were set at 10 accumulations of 6 s with a laser power reaching 50%. In some cases, the total measuring time and laser power were modified (e.g. 20 accumulations of 3 s at 50% or 20% laser power; 10 accumulations of 6 s at 20% laser power) to avoid detector saturation. The objective lens has a 5.9 mm working distance and a light-blocker with a protective foam was slid over the probehead. The spot size is less than 0.5 mm (measured with the light blocker). No post-calibration of the data was performed but the system was checked on the field and prior to the analysis using sulphur (UCB) and cyclohexane (Kaiser).

2.1.3 The RaPort handheld Raman analyzer (EnSpectr, San José CA, USA)

The EnSpectr RaPort Raman spectrometer is equipped with a frequency-doubled Nd:YAG laser with a wavelength of 532 nm. The maximum output power is 30 mW. To avoid thermal damage to the organic colorants, the laser power was lowered via software between 20 and 50% of the maximum. The instrument is handheld, with a weight of 2.5 kg. During the measurement session, the power was supplied by the internal battery, allowing wireless operation up to 6 h. The measurement range is fixed but very wide, from 125 to 4070 cm^{-1} , with a maximum spectral resolution of 7 cm^{-1} . The minimum spot size is 0.5 mm. No calibration is required before measurements. Measurement time ranged from 10 to 30 s per spectrum. The instrument is USB-connected to a laptop, where the spectra are visualized and saved in ASCII format for identification and processing.

2.2 Laboratory measurements

2.2.1 Micro-Raman spectroscopy

Micro-Raman analysis was performed on all the samples taken during the on-site campaign, without further preparation, and on cross-sections embedded in resin obtained from three samples. Non-polarized Raman spectra were recorded at 632.8 nm (He–Ne laser) in a nearly backscattering geometry with a Horiba LabRam microspectrometer equipped with an integrated Olympus BX40 microscope. The spectral resolution was about 2 cm^{-1} . The power on the sample was kept under 10 mW using neutral density filters. A 100X objective was used to collect the Raman signal, with a space resolution of 1 μm . A Raman profile containing 20 points with 2 μm of step was obtained on a selected cross-section.

2.3 Software

All data acquisition was performed with software provided by the manufacturers. Post manipulation of the in situ Raman spectra was performed with OPUS™ software (Bruker) and Thermo Grams/AI 8.0® suite software (Thermo Fischer Scientific). Horiba LabSpec 5 was used for the acquisition and processing of the micro-Raman maps.

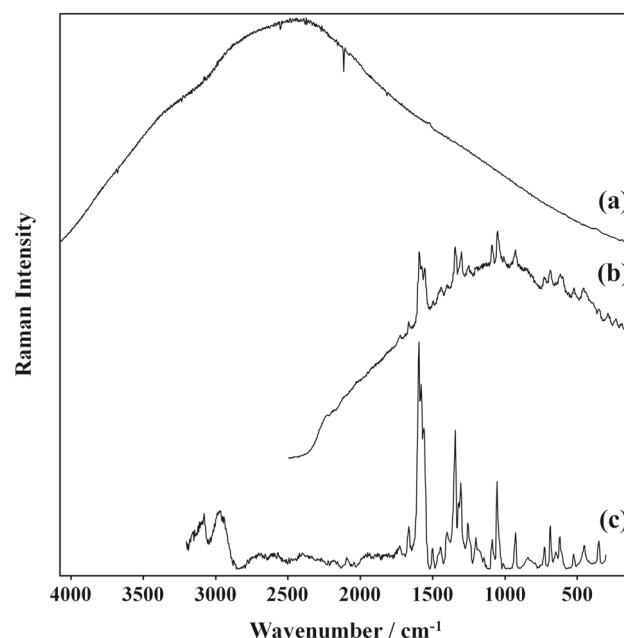
3 Results and discussion

3.1 In situ Raman spectroscopy: issues and comparison of the instruments

For the purpose of the analysis of the street art belonging to the Cooperative Popular Houses of Mancasale and Coviolo in Reggio Emilia (Italy), three mobile Raman spectrometers, coupled to different laser excitations were brought to the field. Although the direct Raman analysis is the optimal approach for characterizing cultural heritage artefacts without jeopardising them, its application is not always straightforward.

The measurements conducted on the murals colourful surfaces were all concluded in one day during the day time. Raman spectroscopy is challenged by light interferences, and thus, the identification of the unknown can be hampered. In Fig. 2a, it is illustrated that the RaPort Raman system suffered light interferences, when measuring a coloured area (red faded to light red) from the ‘Big Sacral Bird’. The excess fluorescence present in the spectrum, made it difficult to identify the synthetic organic pigment present on the painting. The *i-Raman*® EX and Bravo Raman spectrometers were able to characterize the main pigment used as the diketopyrrolo-pyrrole (DPP) pigment PR254 (Fig. 2 b, c and Table 1).

Fig. 2 Representative Raman spectra of the red faded to light red area of the outdoor mural ‘Big Sacral Bird’ collected with the **a** the handheld Raman analyzer *RaPort*, **b** dispersive *i-Raman*[®]EX portable system (PR254) and **c** the *Bravo* handheld Raman spectrometer (PR254)



When measuring in situ, ambient light interferences can be avoided by ensuring dark conditions between the Raman probehead of the spectrometer and the surface under study. In general, this can be achieved either by measuring at night or in dark conditions, e.g. measuring in light-blocking tents, switching off the lights when measuring in museums, etc. In this case, dark conditions were created by bringing the probeheads in complete contact with the surfaces. For the *i-Raman*[®]EX Raman spectrometers, the long fibre optics probehead can easily reach any distant surface and by sliding a light-blocker cup with a protective foam over the probehead (Fig. 1d) the darkened measuring conditions can be met. Indeed, in none of the spectra collected with this mobile system from the three street art murals, light interferences were observed. In the case of *RaPort* and *Bravo* Raman systems, these are coupled to fixed optical heads (Fig. 1e). Although in the *Bravo* data, no major interferences were observed, in several spectra from *RaPort* the daylight was reflected in the spectra. Spectra of *Bravo* seem unaffected to these interferences as these are effectively eliminated by the sequentially shifted excitation algorithm that the spectrometer uses to treat and produce the final spectrum.

Regarding the fluorescence observed, in general, this is unavoidable and it is a phenomenon inherited in Raman spectroscopy. One can use higher laser wavelengths to try to avoid electronic transitions, hence minimise the fluorescence emission. However, by increasing the wavelength, the decreasing of the Raman scattering is expected. *RaPort* is equipped with a 532 nm laser, a wavelength that often is ideal for resonance Raman spectroscopy [46]. Several components of the coloured surfaces of the murals were identified by using the 532 nm laser, thanks to the resonance of some pigments. Unfortunately, in some cases, fluorescence was overwhelming the Raman signals. In general, as better evidenced in the following, for the analysis of mural paintings the advantage of having a better efficiency by using a short-wavelength (e.g. 532 nm) laser, does not compensate for the big disadvantage of inducing too much fluorescence. The 1064 nm laser of the *i-Raman*[®]EX worked adequately in most of the cases with the materials characterization, although fluorescence still occurred in some cases. Moreover, in order to achieve an acceptable *signal-to-noise* ratio in a short measurement time, the *i-Raman*[®]EX was operated at 50% of its maximum power. The same situation was valid when using the *RaPort* spectrometer: a compromise between short acquisition time (essential when using a handheld instrument without tripods or other supports) and a good *signal-to-noise* ratio, would require the use of elevated laser power. However, excessive power can cause alteration to the measured material, which could be observed as the Raman signal of the colorant was decreasing when increasing laser power, evidencing their photo-degradation [47–49]. So the careful choice of the laser power when analysing different colours (different light absorption) was highly important.

To eliminate fluorescence or signals other than the Raman bands, *Bravo* uses the sequentially shifted excitation technology. For each laser (785 and 853 nm), the instrument acquires three spectra in slightly different excitations in order to reconstruct two fluorescence-free spectra, that are finally merged to a single final spectrum. Indeed, *Bravo* produced the best results from the mobile Raman systems used in this study and was able to measure all of the high- and most of the low-intensity bands for the components present on the surfaces. Drawbacks of the system are the non-flexible probehead and the fixed total laser power used. Moreover, although this handheld Raman spectrometer can be easily operated by a non-expert, the interpretation of its data is sometimes challenging. One should always cross-check the final spectrum with the raw data, to check for possible spectral artefacts: in some measurements, the algorithm produced an erroneous and difficult to interpret final spectrum.

From all the aforementioned, the necessity of collecting data with several Raman instruments using different lasers and technologies is underlined. Specifically, from the in situ measurements conducted on the outdoor street art murals belonging to the

Table 1 Overview of the street art murals' colours together with their materials identification, for all the mobile Raman systems discussed in the study. The colours fading is indicated (when possible) in the colour column. The band positions are referring to the Bravo handheld Raman system and are assigned according to [29–31, 33, 52, 53]. Particular assignments with other Raman systems/lasers are underlined in the band positions column. The band positions in brackets denote unresolved bands. +, positive identification; x, no identification

Colour	Bands positions (cm^{-1})	Identification	Bravo	1064 nm	532 nm
<i>Big Sacral Bird</i>					
Red faded to light red	1664, 1593, 1579, 1561, 1498, 1443, 1400, 1344, 1318, 1305, 1254, 1201, 1088, 1052, 1012, 926, 726, 685, 644, 620, 522, 451, 351	PR254	+	+	1523 cm^{-1} with low-frequency weak bands
Orange faded to pink	1667, 1595, 1522, 1510, 1447, 1403, (1349) 1329 (1297), 1262, 1159, 1125, 1089, 1066, 1042, 1016, 953, 918, 844, 824, 802, 778, 644, 357, 318	PY74	+	+	+
	610, 447	Rutile	+	+	x
	985	Barite?	+	+	x
Orange-red faded to brown	1596, 1539, 1475, 1420, 1336, (1297) 1273, 1240, 1158, 1088, 1047, 1000, 916, 768, 668, 386, 538, 370	PO34	+	1592 cm^{-1}	1596 cm^{-1}
	610, 447	Rutile	+	x	x
Lemon yellow faded to pale yellow	1668, 1594, 1549, 1510, 1458, 1439, 1404, 1352, 1329, 1299, 1264, 1160, 1089, 1067, 1044, 1018, 952, 916, 846, 825, 801, 781, 740, 644, 403, 359, 319	PY74	+	+	+
	613, 447	Rutile	+	+	x
Deep blue (stable colour)	1642, 1588, 1431, 1390, 1346 (1334), 1255, 1208, 1167, 1148, 1108, 993, 950, 932, 920, 747, 723, 670, 618, 590, 527, 485, 414, 317	PV23	+	+	+
	1530	PB15	+	+	x
Orange-red faded to light purple	1653, 1596, 1539, 1476, 1420, 1338, (1291) 1274, 1238, 1159, 1086, 1048, 1000, 915, 776, 768, 668, 536, 369	PO34	+	+	ca. 1596 cm^{-1} with a non-identified bands pattern
	610, 447	Rutile	+	+	x
Military green (stable colour)	1596, 1530, 1452, 1342, 1308, 1254, 1214, 1188, 1144, 1109, 1008, 952, 746, 680, 482	PB15	+	1592, 1523 cm^{-1}	x, non-identified bands pattern below ca. 1200 cm^{-1}
	611, 449	Rutile	+	x	+
	821, (358) 336	Bismuth vanadate	+	Broad features	x

Table 1 continued

Colour	Bands positions (cm ⁻¹)	Identification	Bravo	1064 nm	532 nm
Gold yellow faded to light brown	1086	(Calcite) ?	+	x	x
	1659, 1596, 1400, 1335, 1289, 1254, 954, 918, 538	PY83	+	+	Not measured
	612, 449	Rutile	+	+	
	822, (362) 337	Bismuth vanadate	+	+	
Red	1670, 1603, 1580, 1552, 1484, 1462, 1390, (1373) 1359, 1332, 1282, 1260, (1242) 1230, 1204, 1162, 1010, 1061, 1040, 966, 892, 865, 812, 744, 726, 679, 616, 571, 527, 467, (442) 430, 389, 346	PR112	+	+	Not measured
<i>The Big Mother</i>					
Blue	1530, 1450, 1342, 1304, 1143, 1109, 1006, 952, 834, 777, 748, 716, 680, 592, 482	PB15	+	Saturation of the detector	+
	1390 (measured with the 532 nm laser)	(PV23) ?	x	Saturation of the detector	+
Blue	1606, 1530, 1450, 1342, 1304, 1143, 1108, 1006, 953, 834, 779, 748, 715, 680, 593, 483	PB15	+	Saturation of the detector	+
	ca. 1387 (measured with the 532 nm laser)	(PV23) ?	x	Saturation of the detector	+
Dark violet	1641, 1588, 1431, 1390, 1347, 1333, 1255, 1208, 1168, 672, 591, 528, 318	PV23	+	+	+
	1086, 712	Calcite	+	+	+
	612, 445	Rutile	+	+	+
<i>The Economy Subdues You</i>					
Orange faded to light yellow	1668, 1598, 1550, 1507, 1454, 1404, 1352, 1328, 1299, 1263, 1160, 1088, 1042, 800, 358	PY74	+	+	+
	610, 447	Rutile	+	+	+
Red faded to purple	1598, 1538, 1476, 1422, 1340, 1274, 1240, 1160, 1080, 1047, 1000, 916, 814, 772, 668, 536, 368	PO34	+	+	1600 cm ⁻¹
	611, 449	Rutile	+	+	x
Orange faded to white	1666, 1596, 1544, 1509, 1460, 1440, 1404, 1350, 1328, 1298, 1263, 1160, 1128, 1086, 1040, 918, 842, 801, 358	PY74	+	+	+
	610, 448	Rutile		+	+
Turquoise faded to light turquoise	1596, 1530, 1451, 1341, 1308, 1210, 1186, 1143, 1108, 1006, 952, 834, 779, 746, 680, 482	PB15	+	+	+
	610, 446	Rutile	+	x	+

Cooperative Popular Houses of Mancasale and Coviolo in Reggio Emilia (Italy), *Bravo* instrument outperformed the other two. The spectra were easily collected as the measurements were conducted on an automatic mode and the materials identification was more complete compared to *i-Raman*[®]*EX* and *RaPort*. The *i-Raman*[®]*EX* better characterized the components of the murals than the *RaPort*, with the latter positioned at the bottom place out of the three.

Although working on unstable scaffolding with direct sunlight were challenging conditions, the different mobile Raman systems were able to characterize the materials found on the surfaces of: the 'Big Sacral Bird' by Kenor, 'The Big Mother' by Gola Hundun and 'The Economy Subdues You' by Zosen. In Table 1, the identification of materials collected from different areas on the murals, with the three mobile systems used, is described together with the identified Raman band positions for each component.

3.2 In situ identification of the chromophores

In all the analysed areas, a suitable dye or pigment was identified, representing the vast majority of the chromophores present in the paintings. The results are summarized in Table 1, with the indication of the instruments able to identify them. In the following, some details of the results obtained on the different paintings are shown.

3.2.1 'Big Sacral Bird' by Kenor

The monoazopigment, acetoacetic arylide PY74 was found on the discoloured surfaces of the 'Big Sacral Bird'. In Fig. 3a, the spectrum of the PY74 of an orange faded to pink area is presented. In this spectrum the bands at 1349 and 1297 cm^{-1} (indicated in Fig. 3a with an *) are unresolved. Although the low spectral resolution of *Bravo* might pose several identification problems on bands found in close spectral proximity, as here the bands have a spectral difference of more than 10–12 cm^{-1} , in this case, the system did not suffer this problem. Thus, other explanations involving a real change in the spectrum should be involved: a small band shift or broadening can be attributed to degradation phenomena that could have occurred naturally (weathering) or due to the laser power. The same unresolved pattern was noticed also in some spectra recorded with the *i-Raman*[®]*EX* system, although this was not frequently observed, as in most cases these bands were resolved. In the spectrum in Fig. 3b, the bands of PY74 seem more resolved compared to the spectrum of Fig. 3a.

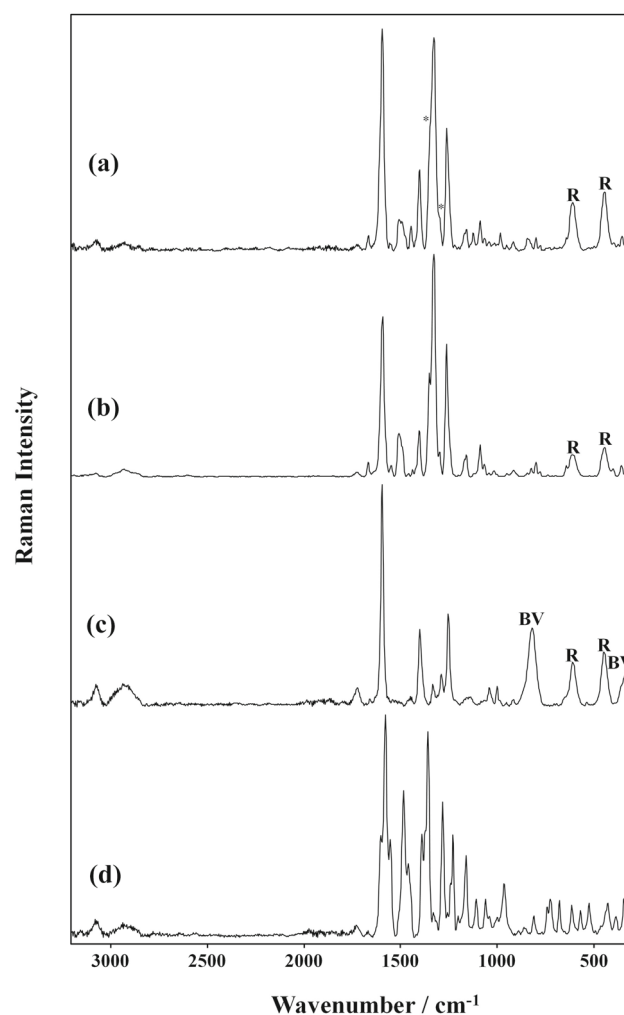
Additional examples of unresolved bands of synthetic organic pigments can be also found in several cases with several Raman systems, with some examples demonstrated in Table 1, and in Figs. 3d, and 4c, d. Again, this might point out to a degradation visualized in the Raman spectra, but the source of the degradation is not straightforward (weathering, photo degradation or post-laser degradation). Ciccola et al. in 2019 [17], when studying the role of SOPs in the degradation of Acrylem AC 33 under UVB, observed certain alterations on the Raman signals before and after exposure. For some SOPs band broadening was observed (while for others not). After averaging spectra collected from Raman mappings and by band fitting, the visualization of changes was possible for the PB 15:1, PG 7 and PR 264 pigments. The Raman bands before and after the degradation experiments were contrasted on the basis of normalization with the unaltered bands. Pause et al. in 2021 [50] evaluated the BRAVO Raman system for the identification of SOPs in varnished paints. Micro-Raman spectroscopy was also used for comparison reasons. The authors, among other aspects regarding Raman spectroscopy in general and the Bravo handheld instrument in particular (fluorescence, spectral resolution, laser-induced damage) are discussing the shift or merge or broadening of the Raman bands, and they attributed that phenomenon to the elevated laser power of the handheld instrument. Although, shifting of the Raman bands may be attributed to other reasons [30, 39]. Moreover, broadening and merging can occur when bands are overlapping, especially in cases of molecular vibrations found on close wavenumbers.

For the murals discussed in the current study, if the spectral resolution is not responsible for the unresolved bands, broadening, shifting, and merging can be the final product of either natural exposure to the outdoor environmental conditions or laser degradation. For the Bravo Raman system, the laser power is fixed (less than 100 mW) with literature reporting that laser powers of 45 mW [50] and 50 mW [51] are reaching the sample surface. For the other mobile Raman systems also elevated lasers powers were used. Shifting of the Raman bands is not only so straightforward as it can arise from natural or laser-induced degradation but also from focusing, stability, calibration, sample form, shape or size of the granules or crystals, etc. so no major conclusions are discussed regarding this aspect in the current study.

According to Scherrer et al. [29], PY74 demonstrates strong vibrations at 1593 and at 1352 cm^{-1} and a very strong band at 1328 cm^{-1} . In a gold yellow faded to light brown area (Fig. 3c) the combination of the disazopigment, diarylide PY83 and bismuth vanadate (BiVO_4) were responsible for the colouring [52, 53]. The phthalocyanine pigment PB15 together with bismuth vanadate were responsible for the shade of one of the measured green colours. The symmetric (Ag) and antisymmetric (Bg) bending modes of bismuth vanadate (BiVO_4) [53] seemed partially unresolved in the current study. Although, the aforementioned reasons may play a role for the unresolved and broad features, this might also be indicative of the presence of monoclinic and tetragonal BiVO_4 [52]. Also, monoclinic and tetragonal BiVO_4 differ on their symmetric V–O stretching mode (Ag symmetry) with tetragonal showing a band at 850 cm^{-1} and monoclinic below 830 cm^{-1} [53–55].

Concerning the red pigments, PR254 (Fig. 2b and c) and the naphthol AS monoazopigment PR112 (Fig. 3d) were positively identified on different areas of the mural, while a disazopigment (pyrazolone PO34) was found for the orange-red faded to brown and

Fig. 3 Representative Raman spectra collected from the street mural ‘Big Sacral Bird’, with the *Bravo* handheld Raman spectrometer, corresponding to **a** an orange faded to pink area (PY74 and rutile (R)), **b** a lemon yellow faded to pale yellow area (PY 74 and rutile (R)) **c** gold yellow faded to light brown area (PY83, bismuth vanadate (BV) and rutile (R)) and **d** a red area (PR112)



light purple areas. In a deep blue area, the polycyclic dioxazine pigment PV23 was positively identified together with the possible incorporation of PB15.

3.2.2 ‘The Big Mother’ by Gola Hundun

PB15 was found in different blue areas measured on the ‘The Big Mother’ mural (Fig. 4a). The *Bravo* Raman system was unable to identify the second pigment present in the mixture. In the data from the blue areas collected from the *RaPort* spectrometer, a band at ca. 1390 cm^{-1} is possibly attributed to the presence of PV23. PV23 is the main colour of the dark violet area measured (Fig. 4b).

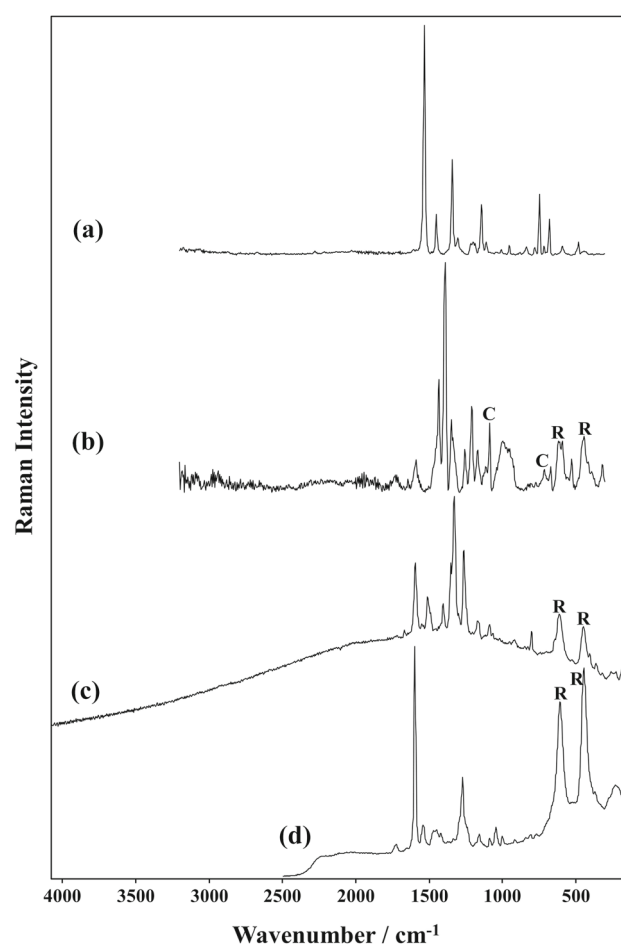
3.2.3 ‘The Economy Subdues You’ by Zosen

PY74 was positively characterized as an orange faded to light yellow (Fig. 4c) and to white areas, respectively. In Fig. 4d the pigment PO34 was found in a red faded to purple area. Pigment PB15 is responsible for the turquoise hue found on the outdoor mural’s surface.

3.2.4 Other components

In most of the areas, measured C-H stretching vibrations were found above 2900 cm^{-1} , while measuring with the *Bravo* instrument. Its extended spectral region (until 3200 cm^{-1}) and the lasers used are ideal for Raman signals found in this spectral area. A band at ca. 1723 cm^{-1} present in many spectra (sometimes together with bands at ca. 1042 and 1002 cm^{-1}) might be due to the resin used [56]. Alkyd and modified alkyd solvent-based spray paints have been mainly employed by the artists, i.e. MTN 94 spray cans, as suggested by archive documentations [9, 43].

Fig. 4 Representative Raman spectra: collected from the mural ‘The Big Mother’ with the Bravo handheld Raman system, corresponding to **a** blue area (PB15), **b** a dark violet area (PV23, calcite (C) and rutile (R)); collected from the mural ‘The Economy Subdues You’ with **c** the RaPort handheld Raman spectrometer, corresponding to an orange faded to light yellow area (PY74 and rutile (R)) and **d** with the dispersive i-Raman[®] EX portable system, corresponding to a red faded to purple area (PO34 and rutile (R))



Calcite (CaCO_3) is positively identified in the spectrum of Fig. 4b while barites (BaSO_4) can be a possible interpretation of the band at 985 cm^{-1} (although downshifted and in absence of other bands) from an orange faded to the pink area (Fig. 3a).

Rutile (TiO_2) is undoubtedly the protagonist in most of the spectra collected from the ‘Big Sacral Bird’ and the ‘The Big Mother’ (only a few did not contain spectral features of rutile) and in all the spectra collected from ‘The Economy Subdues You’. As mobile Raman spectroscopy is a surface-sensitive technique, by using in situ analysis it is not possible to determine whether the TiO_2 originates from the paint mixtures or whether it migrated to the surface from an underlying layer. The migration of rutile is a phenomenon that has been demonstrated before on outdoor street murals [9, 57]. Possible answers to the presence of rutile were given with the help of micro-Raman spectroscopy performed on cross-sections.

3.3 Analysis of degradation and fading

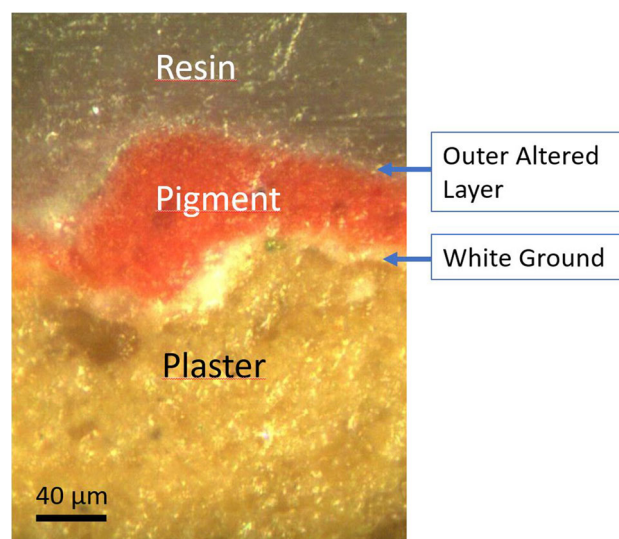
The four investigated artworks, exposed to extreme sunlight and weather conditions, are characterized by visible chromatic alterations and problems of cracking with flaking and losses with the crack pattern that follows the bricks underneath.

‘The Big Mother’ by Gola Hundun, the ‘Big Sacral Bird’ by Kenor, the ‘Oriental Carpet’ by H101 and ‘The Economy Subdues You’ by Zosen are exposed to sunlight and weather. In ‘The Economy Subdues You’, the most exposed of the murals (absence of trees and south orientation), the general fading is more evident than in other artworks. In two artworks (by Kenor and H101), there are also visible problems of cracking with flaking and losses with the crack pattern that follows the bricks underneath.

In locations where the prime coating is absent, the damage is slightly more severe, with pronounced cracks, larger flakes, and in the lower part, also subfluorescence between the ground layer and the plaster.

During the condition report compilation and the photographic documentation, recurring alterations on some colors emerged. For example, an orange color used in three artworks has turned into greyish purple. Some orange, purple and yellow colours faded partially, while a dark pink used in almost every artwork disappeared completely.

Fig. 5 Microscope image of the cross-section obtained on the altered light pink-purple area of ‘Oriental Carpet’. From bottom to top: plaster, white ground layer, thick orange pigment layer, thin pink altered layer



3.3.1 Micro-Raman spectroscopy

During the measurement campaign performed with mobile instruments, a few millimetre-size painting samples were taken on positions subject to the major colour changes to be studied with micro-Raman, in order to understand the fading mechanism.

Micro-Raman analyses have been carried out on all the samples, without further preparation, showing the same pigments detected with the mobile spectrometers. The rutile underlayer was detected in almost all samples, allowing to better understand the stratigraphy of the painting. From 3 samples (one for each painting, except “The Big Mother”) showing the most evident fading issues, cross-sections were obtained. In all cases, the point-to-point micro-Raman analysis showed a similar situation: a rutile underlayer, a painting layer containing one or more dyes and minor rutile, and a very thin outer layer with rutile and a small amount of dye. To better understand this phenomenon, a linear Raman micro-map was carried out on the sample “H101” taken from “oriental Carpet”, selected as representative for its clear stratigraphy and its big change in hue.

3.3.1.1 ‘Oriental Carpet’ by H101 The sample “H101” (from the name of the artist) comes from a light pink-purple area of the ‘Oriental Carpet’ painting. From the photographic record, it is evident that the original hue was an intense orange-red. The cross-section (Fig. 5) reveals the presence of a thin, white ground layer (less than 10 μm) over the plaster, then a thicker vivid orange layer, with variable thickness (average value of *ca.* 40 μm) and a very thin greyish outer layer (few μm).

Although a limited number of in situ measurements were performed with all the mobile Raman instruments, we are able to confirm the presence of PO34 and rutile in the particular area discussed here. In general, rutile was identified in most of the measured areas.

Micro-Raman measurements, performed in different points of the three layers, demonstrated the presence of rutile in the ground layer and of PO34 in the orange layer, together with a minor amount of rutile. The outer layer, which is clearly related to the faded colour, contains mostly rutile, with minor concentrations of PO34. To better follow the relative concentrations of the two compounds, a micro-Raman profile was obtained along the cross-section, from plaster to the outer layer (Fig. 6a and b). The Raman profile clearly shows how the amount of rutile (marked with ‘R’), maximum in the white preparation layer, increases from the orange layer to the outer grey one. On the contrary, the signal of PO34 (marked with ‘P’) decreases significantly from the orange layer to the outer one.

The fading is related to the relative enrichment of rutile in the outer layer. Two possible mechanisms could explain this phenomenon. The first one is the photo-degradation of PO34 due to the exposition of the sunlight, depleting the outer layer and producing a local higher concentration of rutile. This is the simplest possible explanation, but this would mean that the lightfastness of PO34 (and many other pigments showing fading in these paintings) is very poor, less than expected. One should take into account the fact that nanocrystalline TiO_2 rutile is an efficient photo-catalyst, able to induce degradation of organic molecules exposed to sunlight [58–61]. The absence of any PO34 degradation products, which have not been found in the outer layer, can be supported by the efficient photocatalytic activity of TiO_2 . PO34 molecules have been locally degraded by the photo-catalyst into volatile species (H_2O , CO_2) which are no longer on the artwork surface.

The second possible explanation is the migration of rutile from the inner layers to the outer surface. The migration seems to start from the inner layer, because the concentration of rutile in the orange layer is very low. The migration could happen through micro-cracks in the paint layers or through diffusive phenomena that need further investigation. Even if this explanation seems more complex, it appears to better correspond to the observations. The migration of rutile particles through a paint layer was already observed by one of the authors during a master thesis work on the degradation of the Klein Blue, presented at different conferences

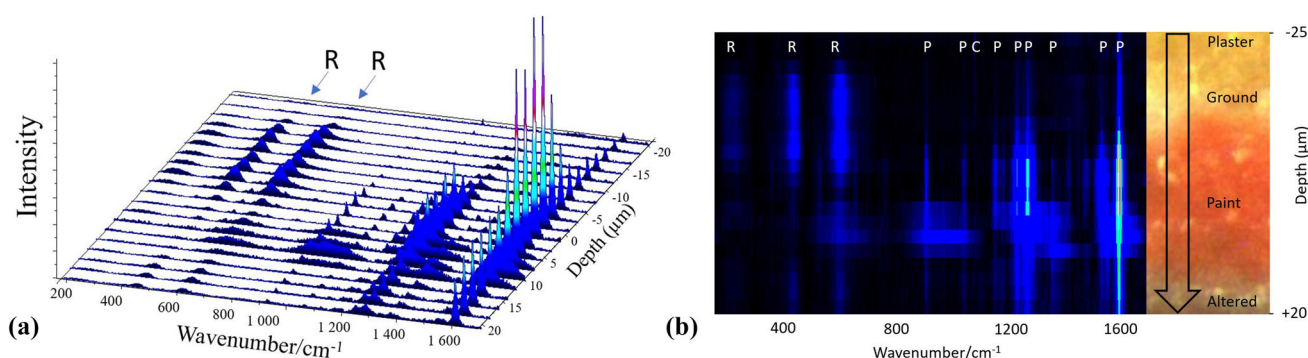


Fig. 6 **a** Linear profile of Raman spectra obtained through the paint layer, of the sample collected from a light pink-purple area, from the plaster (depth $-20\ \mu\text{m}$), through the white ground layer (from -15 to $-5\ \mu\text{m}$ nearly) and the paint layer (-5 to $15\ \mu\text{m}$ nearly) to the outer altered layer (from 15 to $20\ \mu\text{m}$). R indicates the main Raman bands of rutile. All the sharp bands at higher wavenumbers are attributed to the PO34; **b** False-colour bi-dimensional representation of a linear profile of Raman spectra obtained through the paint layer of the sample (collected from a light pink-purple area) with a microscope picture of the analysed area. In the Raman profile, the lightness is proportional to the Raman signal. R = rutile, C = calcite (of the plaster), P = PO34

(e.g. Sodo et al. Non-destructive and Microanalytical Techniques in Art and Cultural Heritage Research Conf., Lisboa 2007) Further studies on artificially aged synthetic paint layers could help to investigate the mechanism at the basis of the migration of rutile and to better quantify the lightfastness of the involved organic dyes. It should be noted that during the last years, the hypothesis of the migration of rutile particles was already invoked in similar cases [9, 57].

4 Conclusions

In situ Raman spectroscopy and micro-Raman spectroscopy were employed to identify the artists' palette and investigate degradation phenomena affecting these colourful works of art. In particular, the three mobile Raman spectrometers employed, allowed us to identify the vast majority of the pigments used and underline the extensive presence of rutile on the murals' surfaces. Micro-Raman spectroscopy performed on selected cross-sections not only confirmed this but was also able to locate the rutile in the stratigraphy. We notice those recent developments in the use of the Raman spectroscopy, in particular of the SORS (Spatially Offset Raman Spectroscopy) technique, could allow to obtain stratigraphic information on paintings without the need for sampling [34].

'The Big Mother' by Gola Hundun, the 'Big Sacral Bird' by Kenor, the 'Oriental Carpet' by H101 and 'The Economy Subdues You' by Zosen are exposed to sunlight and weather. In 'The Economy Subdues You', the most exposed of the murals (absence of trees and south orientation), the general fading is more evident than in other artworks. In two artworks (by Kenor and H101), there are also visible problems of cracking with flaking and losses with the crack pattern that follows the bricks underneath.

In locations where the prime coating is absent, the damage is slightly more severe, with pronounced cracks, larger flakes, and in the lower part, also subfluorescence between the ground layer and the plaster.

During the condition report compilation and the photographic documentation, recurring alterations on some colors emerged. For example, an orange color used in three artworks has turned into greyish purple. Some orange, purple and yellow colours faded partially, while a dark pink used in almost every artwork disappeared completely.

Taking into account the higher damages, in terms of changes of hue and cracking, experienced by the paintings with higher solar exposition and the results obtained on the stratigraphic section, it is possible to hypothesize that the alterations present are mostly due to the disappearance of the organic pigments present in the spray products (first microns) of the paint layer, leaving the TiO₂-based extender and therefore returning a gray-violet tone in some cases (due to the underlying orange color still present) or in many other cases a white background. This provides interesting information on spray products and is of great use for their conservation. It can also be used by artists, to avoid unstable tints or use other types of colors such as quartz dispersion or acrylic-siloxane paints. Moreover, the micro-Raman stratigraphic analysis suggests that a second mechanism, the migration of rutile from the ground layer to the surface, can also play an important role in the fading process. In order to understand the relevance of this phenomenon, further investigations are required.

Supplementary Information The online version contains supplementary material available at <https://doi.org/10.1140/epjp/s13360-022-02423-1>.

Acknowledgements This work was supported by the project "Conservation of Art in Public Spaces (CAPuS)", funded by the European Commission, Programme Erasmus Plus—Key Action 2: Cooperation for innovation and the exchange of good practices—Knowledge Alliances (Call EAC/A03/2016), Project N° 588082-EPP-A-2017-1-IT-EPPKA2-KA. The European Commission's support for the production of this publication does not constitute an endorsement of the contents, which reflect the views only of the authors, and the Commission cannot be held responsible for any use which may be made of the information contained therein. Anastasia Rousaki greatly acknowledges the Research Foundation-Flanders (FWO-Vlaanderen) for her postdoctoral

fellowship with project number: 12X1919N. The authors would also like to thank Ylenia Cobelli for her help during the on-site analysis of the outdoor mural paintings and data interpretation, as these were parts of her degree thesis.

Data Availability Statement This manuscript has associated data in a data repository. [Authors' comment: Data associated with the present work and other investigations related to the CAPuS project can be found at <https://www.capusrepository.unito.it/>. The datasets generated and analysed during the current study are available from the corresponding author on reasonable request.]

Open Access This article is licensed under a Creative Commons Attribution 4.0 International License, which permits use, sharing, adaptation, distribution and reproduction in any medium or format, as long as you give appropriate credit to the original author(s) and the source, provide a link to the Creative Commons licence, and indicate if changes were made. The images or other third party material in this article are included in the article's Creative Commons licence, unless indicated otherwise in a credit line to the material. If material is not included in the article's Creative Commons licence and your intended use is not permitted by statutory regulation or exceeds the permitted use, you will need to obtain permission directly from the copyright holder. To view a copy of this licence, visit <http://creativecommons.org/licenses/by/4.0/>.

References

1. M. Melchiorre Di Crescenzo, E. Zendri, M. Sánchez-Pons, L. Fuster-López, D.J. Yusá-Marco, *Polym. Degrad. Stab.* **107**, 285 (2014). <https://doi.org/10.1016/j.polymdegradstab.2013.12.034>
2. M. Sánchez-Pons, W. Shank, and L. Fuster-López, editors, *Conservation Issues in Modern and Contemporary Murals* (Cambridge Scholars Publishing, Newcastle upon Tyne, NE6 2PA, UK, 2015).
3. E. Ghelardi, I. Degano, M.P. Colombini, J. Mazurek, M. Schilling, H. Khanjian, T. Learner, *Dye. Pigment.* **123**, 396 (2015). <https://doi.org/10.1016/j.dyepig.2015.07.029>
4. J. La Nasa, S. Orsini, I. Degano, A. Rava, F. Modugno, M.P. Colombini, *Microchem. J.* **124**, 940 (2016). <https://doi.org/10.1016/j.microc.2015.06.003>
5. V. Pintus, S. Wei, M. Schreiner, *Microchem. J.* **124**, 949 (2016). <https://doi.org/10.1016/j.microc.2015.07.009>
6. M. Chatzidakis, *Stud. Conserv.* **61**, 17 (2016). <https://doi.org/10.1080/00393630.2016.1201757>
7. C. Santabàrbara, *Opus Quad. Di Stor. Archit. Restauro Disegno=journal Hist. Archit. Conserv. Draw. Nuova Ser.* **2**, 147 (2018). <https://doi.org/10.36165/2147>
8. G. Revista, *Ge-Conservacion* **10**, 77 (2020). <https://doi.org/10.37558/gec.v10i0.731>
9. Bosi, A. Ciccola, I. Serafini, M. Guiso, F. Ripanti, P. Postorino, R. Curini, and A. Bianco, *Spectrochim. Acta - Part A Mol. Biomol. Spectrosc.* **225**, (2020). <https://doi.org/10.1016/j.saa.2019.117474>
10. CAPuS Project. <http://www.capusproject.eu/>. Accessed 14 December 2021.
11. Glossary – CAPuS. <https://www.capusproject.eu/glossary/>. Accessed 17 December 2021.
12. Cooperativa di Abitanti Mancasale e Coviolo. <https://ccpmc.it/>. Accessed 14 December 2021.
13. CAPuS Project. Conservation of Art in Public Spaces (ERASMUS+, Alleanze per la conoscenza) e la conservazione delle opere di street art a Reggio Emilia. <https://ccpmc.it/il-progetto-capus/>. Accessed 14 December 2021.
14. ESPOARTE Contemporary Art Magazine. ¡MURALES!. GLI ARTISTI DI PROYECTO RITUAL ALLE CASE OPERAIE DI MANCASALE. <https://www.espoarte.net/arte/murales-gli-artisti-di-proyecto-ritual-alle-case-operaie-di-mancasale/>. Accessed 14 December 2021.
15. Lascia il segno: Street art, graffiti, murales in Italia e nel mondo. Reggio Emilia: ¡MURALES! Gli Artisti di Proyecto Ritual alle Case Operaie di Mancasale. <https://www.lasciailesegno.it/index.php?it/22/archivio-eventi/280/reggio-emilia-murales-gli-artisti-di-proyecto-ritual-alle-case-operaie-di-mancasale>. Accessed 14 December 2021.
16. J. La Nasa, B. Campanella, F. Sabatini, A. Rava, W. Shank, P. Lucero-Gomez, D. De Luca, S. Legnaioli, V. Palleschi, M.P. Colombini, I. Degano, F. Modugno, *J. Cult. Herit.* **48**, 129 (2021). <https://doi.org/10.1016/j.culher.2020.11.016>
17. A. Ciccola, I. Serafini, M. Guiso, F. Ripanti, F. Domenici, F. Sciubba, P. Postorino, A. Bianco, *Polym. Degrad. Stab.* **159**, 224 (2019). <https://doi.org/10.1016/j.polymdegradstab.2018.11.027>
18. C. Jost, C. Muehlethaler, G. Massonnet, *Forensic Sci. Int.* **258**, 32 (2016). <https://doi.org/10.1016/j.forsciint.2015.11.001>
19. Z.E. Papliaka, K.S. Andrikopoulos, E.A. Varela, *J. Cult. Herit.* **11**, 381 (2010). <https://doi.org/10.1016/j.culher.2010.02.003>
20. E.M. Alonso-Villar, T. Rivas, J.S. Pozo-Antonio, *Prog. Org. Coatings* **154**, 106180 (2021). <https://doi.org/10.1016/j.porgcoat.2021.106180>
21. M. Anghelone, V. Stoytschew, D. Jembrih-Simbürger, M. Schreiner, *Microchem. J.* **139**, 155 (2018). <https://doi.org/10.1016/j.microc.2018.02.029>
22. D. Magrini, S. Bracci, E. Cantisani, C. Conti, A. Rava, A. Sansonetti, W. Shank, M. Colombini, *Spectrochim. Acta Part A Mol. Biomol. Spectrosc.* **173**, 39 (2017). <https://doi.org/10.1016/j.saa.2016.08.017>
23. J. Jehlička, A. Culka, D. Bersani, P. Vandenabeele, *J. Raman Spectrosc.* **48**, 1289 (2017). <https://doi.org/10.1002/jrs.5214>
24. C. Finocchiaro, A. Culka, J. Jehlička, L. Fornasini, A. Rousaki, P. Vandenabeele, *J. Raman Spectrosc.* (2021). <https://doi.org/10.1002/jrs.6278>
25. F. Kosek, A. Culka, L. Fornasini, P. Vandenabeele, A. Rousaki, J. Mirao, D. Bersani, A. Candeias, J. Jehlička, *J. Raman Spectrosc.* **51**, 1186 (2020). <https://doi.org/10.1002/jrs.5873>
26. G. Barone, D. Bersani, J. Jehlička, P.P. Lottici, P. Mazzoleni, S. Raneri, P. Vandenabeele, C. Di Giacomo, G. Larinà, *J. Raman Spectrosc.* **46**, 989 (2015). <https://doi.org/10.1002/jrs.4649>
27. P. Vandenabeele, L. Moens, H.G.M. Edwards, R. Dams, *J. Raman Spectrosc.* **31**, 509 (2000). [https://doi.org/10.1002/1097-4555\(200006\)31:6%3c509::AID-JRS566%3e3.0.CO;2-O](https://doi.org/10.1002/1097-4555(200006)31:6%3c509::AID-JRS566%3e3.0.CO;2-O)
28. P. Ropret, S.A. Centeno, P. Bukovec, *Spectrochim. Acta - Part A Mol. Biomol. Spectrosc.* **69**, 486 (2008). <https://doi.org/10.1016/j.saa.2007.03.050>
29. N.C. Scherrer, Z. Stefan, D. Francoise, F. Annette, K. Renate, *Spectrochim. Acta - Part A Mol. Biomol. Spectrosc.* **73**, 505 (2009). <https://doi.org/10.1016/j.saa.2008.11.029>
30. W. Fremout, S. Saverwyns, *J. Raman Spectrosc.* **43**, 1536 (2012). <https://doi.org/10.1002/jrs.4054>
31. SOPRANO Spectral Library. <https://soprano.kikirpa.be/>. Accessed 14 December 2021.
32. F. Schulte, K.-W. Brzezinka, K. Lutzenberger, H. Stege, U. Panne, *J. Raman Spectrosc.* **39**, 1455 (2008). <https://doi.org/10.1002/jrs.2021>
33. C. Cucci, G. Bartolozzi, M. De Vita, V. Marchiafava, M. Piccolo, F. Casadio, *Appl. Spectrosc.* **70**, 186 (2016). <https://doi.org/10.1177/0003702815615346>
34. A. Botteon, C. Colombo, M. Realini, S. Bracci, D. Magrini, P. Matousek, C. Conti, *J. Raman Spectrosc.* **49**, 1652 (2018). <https://doi.org/10.1002/jrs.5445>
35. L.B. Brostoff, S.A. Centeno, P. Ropret, P. Bythrow, F. Pottier, *Anal. Chem.* **81**, 6096 (2009). <https://doi.org/10.1021/ac9004953>
36. S.Q. Lomax, *J. Coat. Technol. Res.* **7**, 325 (2010). <https://doi.org/10.1007/s11998-009-9205-1>
37. S. Saverwyns, *J. Raman Spectrosc.* **41**, 1525 (2010). <https://doi.org/10.1002/jrs.2654>

38. J. Russell, B.W. Singer, J.J. Perry, A. Bacon, *Anal. Bioanal. Chem.* **400**, 1473 (2011). <https://doi.org/10.1007/s00216-011-4822-9>
39. C. Defeyt, P. Vandenabeele, B. Gilbert, J. Van Pevenage, R. Cloots, D. Strivay, *J. Raman Spectrosc.* **43**, 1772 (2012). <https://doi.org/10.1002/jrs.4125>
40. C. Defeyt, J. Van Pevenage, L. Moens, D. Strivay, P. Vandenabeele, *Spectrochim. Acta - Part A Mol. Biomol. Spectrosc.* **115**, 636 (2013). <https://doi.org/10.1016/j.saa.2013.04.128>
41. M. Vagnini, F. Gabrieli, A. Daveri, D. Sali, *Spectrochim. Acta - Part A Mol. Biomol. Spectrosc.* **176**, 174 (2017). <https://doi.org/10.1016/j.saa.2017.01.006>
42. S. Steger, H. Stege, S. Bretz, O. Hahn, *J. Cult. Herit.* **38**, 20 (2019). <https://doi.org/10.1016/j.culher.2019.01.011>
43. G. Germinario, I.D. van der Werf, L. Sabbatini, *Microchem. J.* **124**, 929 (2016). <https://doi.org/10.1016/j.microc.2015.04.016>
44. A. Ciccola, M. Guiso, F. Domenici, F. Sciubba, A. Bianco, *Polym. Degrad. Stab.* **140**, 74 (2017). <https://doi.org/10.1016/j.polymdegradstab.2017.04.004>
45. N. Sundberg, R. Pause, I.D. van der Werf, A. Astefanei, K.J. van den Berg, M.R. van Bommel, *Microchem. J.* **170**, 106708 (2021). <https://doi.org/10.1016/j.microc.2021.106708>
46. D.A. Long, *The Raman Effect: A Unified Treatment of the Theory of Raman Scattering by Molecules* (Wiley, Chichester, England, 2002)
47. L. Burgio, R.J.H. Clark, S. Firth, *Analyst* **126**, 222 (2001). <https://doi.org/10.1039/b008302j>
48. A. Athanassiou, A.E. Hill, T. Fourier, L. Burgio, R.J.H. Clark, *J. Cult. Herit.* **1**, 209 (2000). [https://doi.org/10.1016/S1296-2074\(00\)00180-1](https://doi.org/10.1016/S1296-2074(00)00180-1)
49. M.A. Rauf, S.S. Ashraf, J. Hazard, *Mater.* **166**, 6 (2009). <https://doi.org/10.1016/j.jhazmat.2008.11.043>
50. R. Pause, I.D. van der Werf, K.J. van den Berg, *Heritage* **4**, 1348 (2021). <https://doi.org/10.3390/heritage4030073>
51. F. Pozzi, E. Basso, A. Rizzo, A. Cesaratto, T.J. Tague Jr., *J. Raman Spectrosc.* **50**, 5585 (2019). <https://doi.org/10.1002/jrs.5585>
52. E.M. Suzuki, *J. Forensic Sci.* **59**, 344 (2014). <https://doi.org/10.1111/1556-4029.12318>
53. M. Gotić, S. Musić, M. Ivanda, M. Šoufek, S. Popović, *J. Mol. Struct.* **744–747**, 535 (2005). <https://doi.org/10.1016/j.molstruc.2004.10.075>
54. B.S. Rodrigues, C.M. Branco, P. Corio, J.S. Souza, *Cryst. Growth Des.* **20**, 3673 (2020). <https://doi.org/10.1021/acs.cgd.9b01517>
55. H.M. Zhang, J.B. Liu, H. Wang, W.X. Zhang, H. Yan, *J. Nanoparticle Res.* **10**, 767 (2008). <https://doi.org/10.1007/s11051-007-9310-y>
56. R. Wiesinger, L. Pagnin, M. Anghelone, L.M. Moretto, E.F. Orsega, M. Schreiner, *Angew. Chemie - Int. Ed.* **57**, 7401 (2018). <https://doi.org/10.1002/anie.201713413>
57. J. Dickens, A. Rava, M.P. Colombini, M. Picollo, W. Shank, *Stud. Conserv.* **61**, 29 (2016). <https://doi.org/10.1080/00393630.2016.1193691>
58. M. Pelaez, N.T. Nolan, S.C. Pillai, M.K. Seery, P. Falaras, A.G. Kontos, P.S.M. Dunlop, J.W.J. Hamilton, J.A. Byrne, K. O'Shea, M.H. Entezari, D.D. Dionysiou, *Appl. Catal. B Environ.* **125**, 331 (2012). <https://doi.org/10.1016/j.apcatb.2012.05.036>
59. J. Schneider, M. Matsuoka, M. Takeuchi, J. Zhang, Y. Horiuchi, M. Anpo, D.W. Bahnemann, *Chem. Rev.* **114**, 9919–9986 (2014). <https://doi.org/10.1021/cr5001892>
60. R. Fagan, D.E. McCormack, D.D. Dionysiou, S.C. Pillai, *Mater. Sci. Semicond. Process.* **42**, 2 (2016). <https://doi.org/10.1016/j.mssp.2015.07.052>
61. V.R. Djokić, A.D. Marinković, R.D. Petrović, O. Ersen, S. Zafeiratos, M. Mitrić, C. Ophus, V.R. Radmilović, D.T. Janačković, A.C.S. Appl. Mater. Interfaces **12**, 33058 (2020). <https://doi.org/10.1021/acsami.0c03150>